Compensatory changes in cellular excitability, not synaptic scaling, contribute to homeostatic recovery of embryonic network activity

Jennifer C. Wilhelm[a], Mark M. Rich[b], and Peter Wenner[a,1]

[a]Department of Physiology, Emory University School of Medicine, Atlanta, GA 30322; and [b]Department of Neuroscience, Cell Biology, and Physiology, Wright State University, Dayton, OH 45435

Edited by Charles F. Stevens, The Salk Institute for Biological Studies, La Jolla, CA, and approved January 30, 2009 (received for review December 24, 2008)

When neuronal activity is reduced over a period of days, compensatory changes in synaptic strength and/or cellular excitability are triggered, which are thought to act in a manner to homeostatically recover normal activity levels. The time course over which changes in homeostatic synaptic strength and cellular excitability occur are not clear. Although many studies show that 1–2 days of activity block are necessary to trigger increases in excitatory quantal strength, few studies have been able to examine whether these mechanisms actually underlie recovery of network activity. Here, we examine the mechanisms underlying recovery of embryonic motor activity following block of either excitatory GABAergic or glutamatergic inputs in vivo. We find that $GABA_A$ receptor blockade triggers fast changes in cellular excitability that occur during the recovery of activity but before changes in synaptic scaling. This increase in cellular excitability is mediated in part by an increase in sodium currents and a reduction in the fast-inactivating and calcium-activated potassium currents. These findings suggest that compensatory changes in cellular excitability, rather than synaptic scaling, contribute to activity recovery. Further, we find a special role for the $GABA_A$ receptor in triggering several homeostatic mechanisms after activity perturbations, including changes in cellular excitability and GABAergic and AMPAergic synaptic strength. The temporal difference in expression of homeostatic changes in cellular excitability and synaptic strength suggests that there are multiple mechanisms and pathways engaged to regulate network activity, and that each may have temporally distinct functions.

development | neurotransmission | plasticity | GABA | glutamate

When network activity is perturbed for days, compensatory changes in cellular excitability and synaptic strength are triggered that are believed to homeostatically recover the original activity levels (homeostatic plasticity, refs. 1–3). A great deal of attention has been focused on compensatory changes in the amplitude of miniature postsynaptic currents (mPSCs) (4, 5). When activity was reduced for 2 days, the amplitudes of excitatory mPSCs were increased across their entire distribution, and this process has been termed synaptic scaling (6). When activity was increased by blocking inhibition, activity levels were homeostatically recovered at some point during the 2 days of inhibitory block. By 2 days, there had been a downward scaling, and it is currently thought that these quantal changes contribute to the recovery of activity levels (5). However, little is actually known about the time course of the recovery process compared with the time course of the mechanisms that are thought to be responsible for this recovery. This comparison is critical to understanding how activity functionally recovers and is then maintained. Previous work suggests that changes in cellular excitability may occur more quickly than changes in quantal amplitude (7, 8). Changes in cellular excitability likely contribute to the recovery of activity, and it remains possible that these changes drive a full recovery before any compensatory changes in quantal amplitude are engaged.

We have identified a form of homeostatic plasticity in the developing spinal cord (9). During development, many networks exhibit a spontaneous network activity (SNA), where many neurons are recruited into episodic bursts of activity (10–12). SNA is produced by hyperexcitable, recurrently connected circuits in which both GABA and glutamate are excitatory. In the developing spinal cord, SNA has been shown to be important for various aspects of limb (13) and motoneuron (14–16) development. We have shown recently that when SNA was reduced for 48 h in vivo, compensatory increases in AMPA and $GABA_A$ quantal amplitude were triggered, suggesting that homeostatic synaptic plasticity contributed to the maintenance of SNA (9).

We have further shown that the compensatory changes in quantal amplitude were triggered through a reduction in $GABA_A$ receptor activation (17). In this way, reductions in GABA binding to its receptor signal that network activity levels have been reduced. This was demonstrated by injecting a $GABA_A$ receptor antagonist in ovo to block GABAergic signaling for 48 h. The injection of the antagonist produced a transient reduction in SNA that homeostatically recovered to control levels within 12 h. Interestingly, this homeostatic recovery of activity occurred before the onset of synaptic scaling.

In this study, we show that reducing $GABA_A$ receptor signaling in vivo for 12 h triggered compensatory changes in cellular excitability in embryonic motoneurons. The findings suggest that fast compensatory changes in cellular excitability appear to recover activity levels, and only after recovery is achieved does synaptic scaling occur, possibly to consolidate changes in network excitability. Increases in cellular excitability were mediated by changes in voltage-gated sodium channel currents as well as transient and calcium-dependent potassium channel currents.

Results

$GABA_A$ Receptor Block Increases Intrinsic Excitability. Blocking $GABA_A$ transmission at embryonic day 8 (E8) reduced embryonic movements, which then recovered within 12 h. Movements (our measure of SNA) were counted during a 5-min observation period (17). This recovery of activity occurred before compensatory increases in quantal amplitude were observed, as described previously (Fig. 1*A*) (17). To determine whether cellular excitability contributed to the recovery of embryonic activity after $GABA_A$ receptor blockade, we treated embryos in ovo for either 12 h (E9.5–E10) or 48 h (E8–E10) with saline, the $GABA_A$ receptor antagonist gabazine, or the glutamate receptor antagonists 6-cyano-7-nitroquinoxaline-2,3-dione disodium (CNQX) and DL-2-amino-5-phosphonopentanoic acid (APV). Solutions were

Author contributions: J.C.W., M.M.R., and P.W. designed research; J.C.W. performed research; J.C.W., M.M.R., and P.W. analyzed data; and J.C.W., M.M.R., and P.W. wrote the paper.

The authors declare no conflict of interest.

This article is a PNAS Direct Submission.

[1]To whom correspondence should be addressed. E-mail: pwenner@emory.edu.

This article contains supporting information online at www.pnas.org/cgi/content/full/0813058106/DCSupplemental.

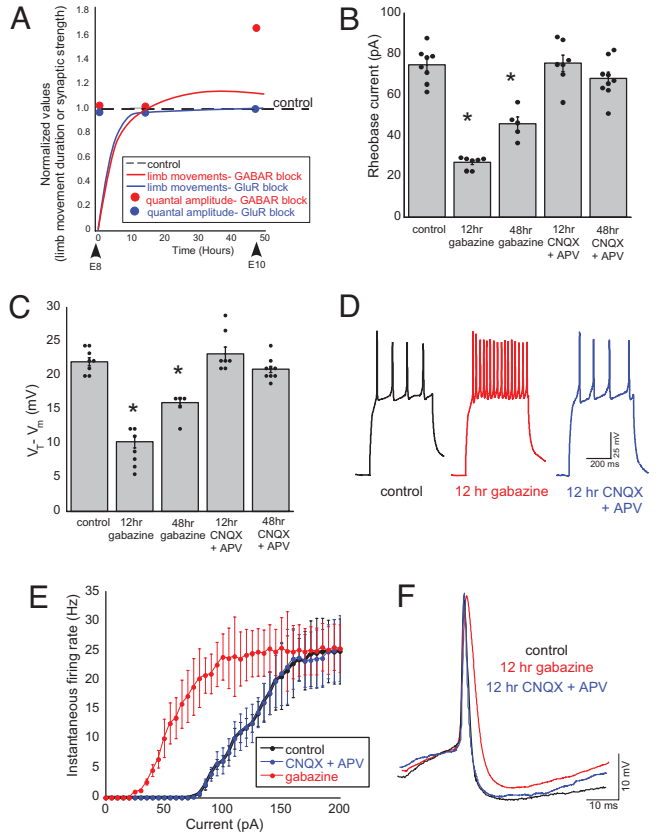

Fig. 1. $GABA_A$ receptor block increased cellular excitability. (*A*) Schematic approximation of the relationship between the recovery of SNA after neurotransmitter block and the subsequent increase in the amplitude of excitatory quantal currents, as shown previously (17). Lines represent an approximation of the duration of limb movements (measure of SNA) for 48 h after the injection of gabazine ($GABA_A$ receptor block) or CNQX plus APV (glutamate receptor block). Values were normalized to control (dashed line). Reducing neurotransmission eliminates limb movements, which then recover in ≈12 h. The amplitude of excitatory quantal currents increased within 48 h after $GABA_A$ receptor block. No change in the amplitude of quantal currents was seen after 48 h of glutamate receptor block or after 12 h of either $GABA_A$ or glutamate receptor block. (*B*) Rheobase current was significantly reduced after $GABA_A$ receptor blockade (*, $P \leq 0.0001$) but not glutamatergic block. (*C*) The average spike threshold ($V_T - V_m$) was reduced after $GABA_A$ (*, $P \leq 0.0001$), but not glutamate, receptor blockade. (*D*) Representative spike trains evoked by somatic current injection (110 pA) in control and treated motoneurons. (*E*) Average f-I curves for control ($n = 5$), gabazine-treated ($n = 8$), and CNQX/APV-treated ($n = 3$) embryos. The 12-h gabazine treatment shifts the average f-I curve to the left, suggesting an increased intrinsic excitability. (*F*) Representative action potentials from control and treated motoneurons. The 12-h gabazine treatment significantly increased spike half-width ($P \leq 0.001$) and decreased the peak of the hyperpolarization ($P \leq 0.05$). Data in this graph and all subsequent graphs are represented as averages ± SEM.

applied to the chorioallantoic membrane through a small window in the shell. At E10, spinal cords were isolated from the embryos, and whole-cell current clamp recordings were obtained from antidromically identified motoneurons. Cellular excitability was initially examined in 2 ways: rheobase current and spike threshold. Rheobase current was determined as the least current necessary to produce an action potential (1-pA step, 500-ms duration). Spike threshold was measured as the difference in voltage between resting membrane voltage (V_m) and the threshold voltage (V_T, voltage evoked by the rheobase current). $GABA_A$ receptor blockade significantly decreased rheobase current and spike threshold in the first 12 h (Fig. 1 *B* and *C* and Table 1). After 48 h of $GABA_A$ receptor blockade, both rheobase current and spike threshold began to return toward control levels (Fig. 1 *B* and *C* and Table 1). These results suggest that $GABA_A$ receptor blockade can trigger changes in cellular excitability that could contribute to the homeostatic recovery of activity.

We previously demonstrated that blocking ionotropic glutamate receptor signaling also produced a transient decrease in SNA in ovo that recovered to control levels at the same rate as $GABA_A$ receptor blockade (Fig. 1*A*). However, blocking glutamate receptors did not result in a change in rheobase current or spike threshold, regardless of the duration of block (Fig. 1 *B* and *C* and Table 1). These results suggest that changes in cellular excitability are not triggered by neurotransmission block in general or the transient activity reduction after antagonist injection.

We next examined cellular excitability by monitoring the firing rates of motoneurons from embryos treated with saline, CNQX/APV, or gabazine for 12 h. Average frequency versus current (f-I) plots were constructed by measuring the instantaneous firing frequency for each current injection. Gabazine-treated motoneurons exhibited a leftward shift in the f-I curve, suggesting that 12 h of $GABA_A$ receptor block increases intrinsic excitability in motoneurons, whereas no such changes were seen following glutamate blockade (Fig. 1 *D* and *E*). Also, the slope of the initial, linear part of the f-I curve was greater for gabazine-treated but not glutamate-treated motoneurons (control, 0.26 ± 0.01 Hz/pA, $n = 5$; CNQX/APV, 0.26 ± 0.03 Hz/pA, $n = 3$; gabazine, 0.34 ± 0.03 Hz/pA, $n = 8$; $P \leq 0.05$).

In addition, gabazine treatment altered various aspects of the action potential, whereas glutamate receptor antagonist treatment did not result in changes (Fig. 1*F*). After 12 h of gabazine treatment, we found an increase in the half-width of the average action potential (control, 3.1 ± 0.1 ms, $n = 8$; CNQX/APV, 2.9 ± 0.1 ms, $n = 3$; gabazine, 5.7 ± 0.2 ms, $n = 8$; $P \leq 0.001$; Fig. 1*F*) and a decrease in the peak of the after-hyperpolarization (control, −6.9 ± 0.4 mV; CNQX/APV, −7.3 ± 0.2 mV; gabazine, −5.5 ± 0.3 mV; $P \leq 0.05$). The peak of the action potential (control, 39.6 ± 0.5 mV; CNQX/APV, 39.4 ± 0.4 mV; gabazine, 39.3 ± 0.4 mV) and the rise time (control, 1.5 ± 0.3 ms; CNQX/APV, 1.6 ± 0.3 ms; gabazine, 1.3 ± 0.2 ms) were not altered by gabazine or CNQX/APV treatment. Further, we found that changes in cellular excitability were not mediated by changes in passive membrane properties, because there were no differences between control and gabazine-treated embryos (Table 1). Together, these findings suggest that 12 h of $GABA_A$ receptor block increased intrinsic excitability in motoneurons, whereas glutamate receptor block did not trigger changes in cellular excitability.

$GABA_A$ Receptor Block Increases Voltage-Activated Sodium Currents. We hypothesized that gabazine-dependent changes in cellular excitability were mediated by changes in voltage-gated channels, as described for other systems (18–20). To test this, we examined voltage-activated sodium, calcium, and potassium currents by using whole-cell voltage clamp recordings from motoneurons of embryos treated for 12 h with saline or gabazine, because this produced the largest changes in rheobase current.

Using a whole-cell voltage clamp, sodium currents (I_{Na}) were elicited by voltage steps from a holding potential of −60 mV. I_{Na} was isolated by using intracellular and extracellular K^+ and Ca^{2+} channel blockers (*SI Methods*). Because our space clamp for I_{Na} was imperfect, we could not generate a reliable activation curve. However, we were able to detect a 92% increase in the peak Na^+ current after gabazine treatment when stepping from −60 mV to −10 mV (Fig. 2). These currents were reduced to 10.3% ± 1.9% of original values by the addition of the Na^+ channel blocker tetrodotoxin (TTX; 1 μM), suggesting that the isolated currents were Na^+ channel-mediated. These results suggest that $GABA_A$ receptor block increases I_{Na}, which could underlie the significant increase in cellular excitability.

Table 1. Motoneuron properties

Treatment condition	n	Rheobase current, pA	Spike threshold, mV	Membrane potential, mV	Input resistance, MΩ	Membrane capacitance, pF
Control	8	74.6 ± 3.0	22.1 ± 0.6	−51.6 ± 0.8	384.1 ± 28.9	20.3 ± 1.5
12 h gabazine	7	28.8 ± 1.1*	10.3 ± 0.9*	−50.3 ± 0.6	337.3 ± 27.2	20.5 ± 1.4
48 h gabazine	5	45.8 ± 3.3*	16.0 ± 0.8*	−53.6 ± 2.6	366.2 ± 14.1	23.6 ± 7.3
12 h CNQX	8	71.8 ± 3.4	20.0 ± 1.3	−50.9 ± 0.6	388.1 ± 15.0	20.3 ± 1.1
48 h CNQX	8	69.8 ± 4.1	20.5 ± 0.8	−51.5 ± 0.7	329.4 ± 20.9	21.8 ± 0.5
12 h CNQX plus APV	7	75.5 ± 4.1	23.1 ± 1.0	−51.9 ± 0.6	383.6 ± 23.7	18.9 ± 1.4
48 h CNQX plus APV	9	67.9 ± 3.2	20.9 ± 0.5	−51.3 ± 0.4	377.8 ± 18.4	19.7 ± 1.2

*, $P \leq 0.0001$

$GABA_A$ Receptor Block Does Not Alter Voltage-Activated Calcium Currents. High-voltage-activated (HVA) calcium currents (I_{Ca}) were measured by applying depolarizing voltage steps to −10 mV from a holding potential of −60 mV. Na^+ and K^+ currents were blocked pharmacologically (see *SI Methods*). The contribution of remaining currents was significantly reduced by subtracting currents elicited in the absence of external Ca^{2+} from corresponding currents when Ca^{2+} was present (10 mM Ca^{2+} − 0 mM Ca^{2+}; Fig. S1). The depolarizing voltage steps produced inward currents that peaked within a few milliseconds and decayed toward a sustained current (Fig. S1 *A* and *B*). Gabazine treatment did not significantly alter the peak Ca^{2+} currents (Fig. S1*C*). Additionally, sustained Ca^{2+} currents, measured 700 ms after the start of the voltage step, were not altered by gabazine treatment (Fig. S1*D*). These data suggested that HVA I_{Ca} did not contribute to the increased cellular excitability following gabazine treatment. Low-voltage-activated calcium currents were not tested.

$GABA_A$ Receptor Block Decreased I_A and $I_{K(Ca)}$. Outward K^+ currents consisted of 2 distinct components: a fast-inactivating, tetraethylammonium (TEA)-insensitive current (I_A) and a sustained current (I_K) likely composed of Ca^{2+}-activated currents (K_{Ca}) and delayed rectifier currents (K_{dr}). These currents were recorded in the presence of TTX; however, Ca^{2+} currents were not blocked to maintain Ca^{2+}-activated K^+ currents.

Applying depolarizing voltage steps from a holding potential of −100 mV to between −30 mV and +50 mV (in 10-mV increments) elicited large outward K^+ currents consisting of I_A and I_K (Fig. 3*A*). I_K could be isolated from I_A when the same voltage steps were preceded by a brief (100-ms) prepulse to −40 mV (Fig. 3*B*), which inactivates I_A in embryonic chick lumbar motoneurons (16, 21). I_A was measured as the peak current resulting from the subtraction of I_K from the total K^+ current (Fig. 3*C*). The addition of external TEA to block I_K did not alter the peak I_A measured, suggesting that we have isolated the TEA-insensitive I_A (control, 4.00 ± 0.03 nA; control plus TEA, 4.03 ± 0.07 nA for steps to +50 mV; $n = 4$). Gabazine treatment significantly reduced I_A (Fig. 3 *D* and *E*) in addition to accelerating I_A inactivation ($P \leq 0.04$; Fig. 3*F*). These changes in I_A would tend to increase cellular excitability and might explain the widened action potential. No change was found in the voltage dependence of I_A (Fig. 3*G*).

Motoneurons treated for 12 h with gabazine had significantly reduced I_K compared with currents from control motoneurons (Fig.

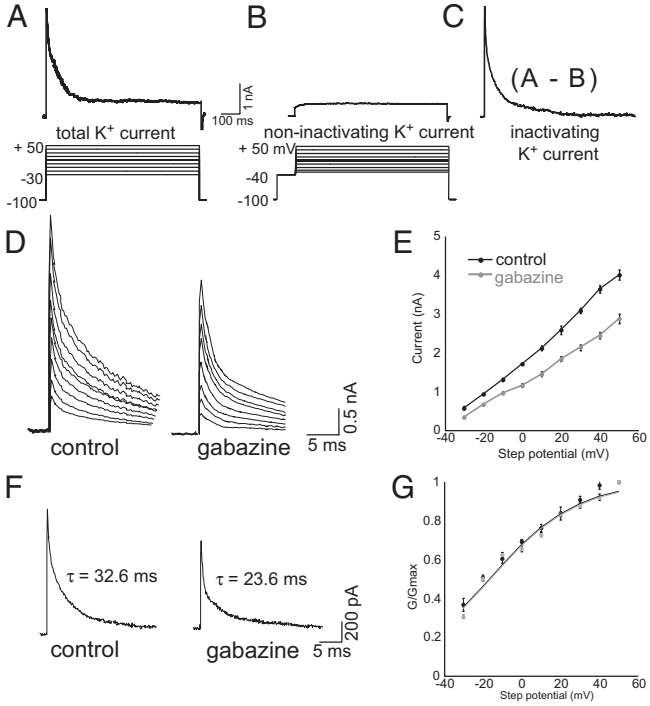

Fig. 3. I_A reduced after 12 h of gabazine treatment. (*A*) Representative total K^+ current elicited by a depolarizing step to +20 mV from a holding potential of −100 mV. The protocol used to evoke total K^+ currents is below. (*B*) Sustained K^+ currents (I_K) were elicited when the same series of voltage steps used in *A* was preceded by a prepulse to −40 mV. A representative I_K trace elicited by a voltage step to +20 mV demonstrates that this current does not rapidly inactivate. (*C*) Difference currents (currents in *B* subtracted from those in *A*) reveal a fast-inactivating K^+ current (I_A). (*D*) The peak I_A currents from control (*Left*) and gabazine-treated (*Right*) motoneurons. (*E*) Gabazine treatment ($n = 11$) significantly reduces I_A currents compared with control ($n = 14$). (*F*) Representative I_A traces evoked by voltage steps to −10 mV from control (*Left*) and gabazine-treated (*Right*) motoneurons with $\tau_{inactivation}$ as indicated. (*G*) Average conductance values normalized to the value at +50 mV produced an approximate activation curve (G/G_{max}) fitted with a Boltzmann equation. Gabazine treatment does not alter the voltage dependence of I_A.

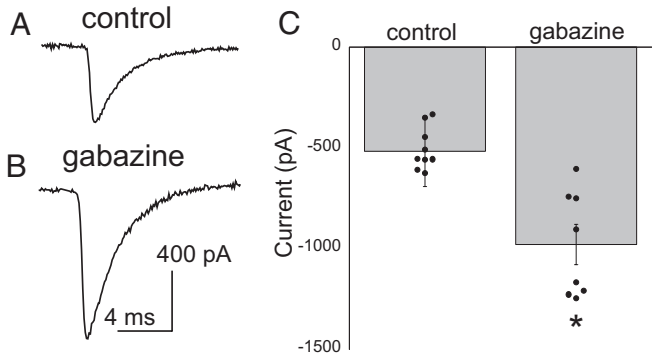

Fig. 2. The amplitude of sodium currents was increased after 12 h of gabazine treatment. Sample traces of Na^+ currents from saline-treated (*A*) and gabazine-treated (*B*) motoneurons elicited by a depolarizing step to −10 mV from a holding potential of −60 mV. (*C*) The average peak current amplitudes elicited by the voltage step to −10 mV from −60 mV were significantly increased after 12 h of $GABA_A$ receptor block (gabazine, $n = 8$; control, $n = 9$; $P \leq 0.001$).

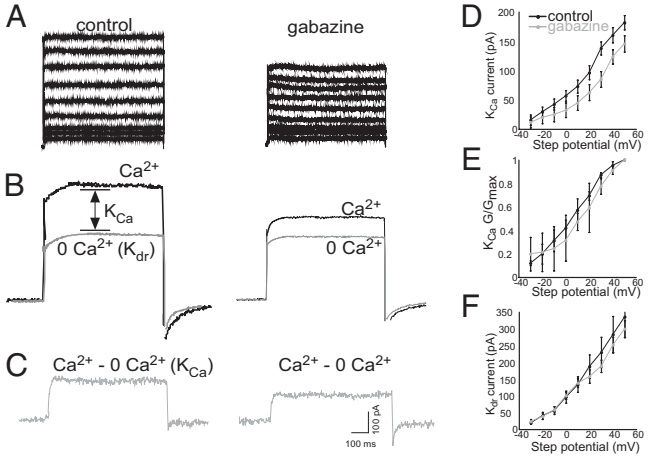

Fig. 4. Gabazine treatment reduces $I_{K(Ca)}$ but not $I_{K(dr)}$. (*A*) Representative I_K evoked by depolarizing steps to +50 mV (in 10-mV increments) from a holding potential of −40 mV. (*B*) Representative currents elicited by a voltage step to +50 mV from a holding potential of −40 mV obtained in the presence and absence of external calcium. K_{dr} is measured as the current evoked in the absence of external calcium. (*C*) Net K_{Ca} currents were obtained after digital subtraction of the raw traces (Ca^{2+} − 0 mM Ca^{2+}). (*D*) Gabazine treatment ($n = 8$) significantly reduced $I_{K(Ca)}$ compared with control ($n = 9$). (*E*) No difference was found in the activation curves from gabazine-treated and control motoneurons. (*F*) Gabazine treatment ($n = 8$) did not significantly alter $I_{K(dr)}$ compared with control ($n = 9$).

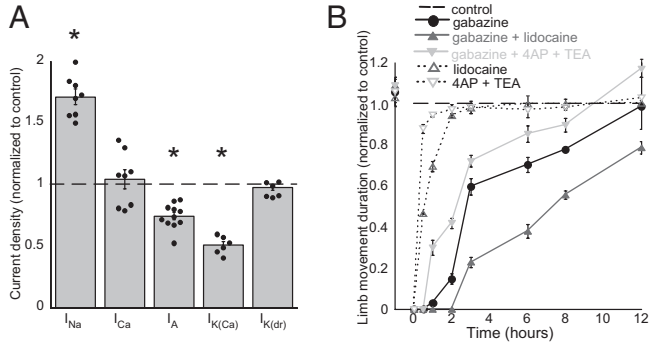

Fig. 5. Changes in current densities observed following gabazine treatment likely contribute to recovery of embryonic movements. (*A*) Average values for gabazine-treated neurons are plotted as a fraction of control (dashed line). Data for I_{Na} and I_{Ca} elicited by a step to −10 mV. Data for I_A, $I_{K(Ca)}$, and $I_{K(dr)}$ were elicited by a step to +50 mV. Currents were normalized to cell capacitance. I_{Na}, I_A, and IK(Ca) were significantly changed (*) in gabazine-treated motoneurons. (*B*) Embryos were injected with a $GABA_A$ antagonist, K^+ channel antagonists, an Na^+ channel antagonist, or a combination of these antagonists, and embryonic movement duration was monitored ($n = 4$, or $n = 3$ when only K^+ or Na^+ channel antagonists were added). Reducing K^+ channel currents accelerated recovery of movements, and reducing Na^+ channel currents slowed recovery of movements.

4 *A* and *B*). Because I_K is composed of $I_{K(Ca)}$ and $I_{K(dr)}$, we assessed the effect of gabazine treatment on $I_{K(Ca)}$ and $I_{K(dr)}$ separately. We used a whole-cell voltage clamp to apply depolarizing steps to +50 mV (in 10-mV increments) from a holding potential of −40 mV (to inactivate I_A). Currents were recorded in a saline solution containing external Ca^{2+} and a Ca^{2+}-free solution (0 mM Ca^{2+}; Fig. 4*B*). $I_{K(Ca)}$ was obtained by digital subtraction (Ca^{2+} − 0 mM Ca^{2+}; Fig. 4*C*). Using this procedure allows the measurement of K_{Ca} currents independently of other currents (16, 21). Gabazine treatment significantly reduced $I_{K(Ca)}$ (Fig. 4*D*). A plot of the mean G/G_{max} values shows considerable overlap between control and gabazine-treated curves (Fig. 4*E*), suggesting that the activation of $I_{K(Ca)}$ is not altered after gabazine treatment. Because HVA I_{Ca} was not altered by gabazine treatment (Fig. S1), the reduction in $I_{K(Ca)}$ in gabazine-treated motoneurons cannot be attributed to a change in Ca^{2+} currents. The decrease in $I_{K(Ca)}$ could explain the reduction in after-hyperpolarization found in action potentials after gabazine treatment. $I_{K(dr)}$ was measured as the amount of current elicited in the Ca^{2+}-free solution (Fig. 4*B*). Removing Ca^{2+} from the external solution allows for measurement of K_{dr} without a contribution from Ca^{2+}-dependent K^+ currents (16, 21). Gabazine treatment did not significantly alter peak K_{dr} currents (Fig. 4*F*).

Activity Recovery Following $GABA_A$ Block Appears to Be Mediated by Changes in Voltage-Gated Current Densities. Individual current measurements were normalized by capacitance before averaging to attain the density of each current. Inward and outward currents were differentially regulated by gabazine treatment (Fig. 5*A*) such that I_{Na} was increased to 178% ($P \leq 0.001$), I_A was reduced to 74% ($P \leq 0.04$), and $I_{K(Ca)}$ was reduced to 51% ($P \leq 0.001$) compared with control. HVA I_{Ca} and $I_{K(dr)}$ remained unaltered. These changes in current density could be due to a change in the number of channels or changes due to properties of single channels; however, no change was observed in the activation kinetics of I_A or $I_{K(Ca)}$.

We reasoned that if the observed changes in current densities underlie the recovery of SNA, then reducing these currents in ovo should influence the recovery process. Embryos were treated with a single bolus of gabazine, gabazine and K^+ channel antagonists 4-aminopyridine (4-AP) and TEA, or gabazine and an Na^+ channel antagonist (lidocaine) at E9.5. We then observed a recovery of embryonic movements in the next 12 h (Fig. 5*B*). Antagonist concentrations were chosen that only slightly influenced embryonic movements when injected by themselves (without gabazine; Fig. 5*B*, dotted lines), suggesting these were submaximal concentrations. We found that reducing K^+ channel currents accelerated the recovery process, whereas reducing Na^+ channel currents slowed the recovery process (Fig. 5*B*). Similar results were observed for the number of bouts of movements and the duration of each bout (Fig. S2). The findings suggested that changes in current densities of Na^+ and K^+ channels influenced the recovery process in a direction that would predict that the changes observed following $GABA_A$ block (reduced K^+ and increased Na^+ channel currents) should facilitate the recovery of activity.

Discussion

Previously, we reported that blocking $GABA_A$ receptor signaling produced a transient reduction in embryonic motor activity that homeostatically recovered to normal levels within 12 h (17). We also found that reductions in GABAergic transmission triggered increases in quantal amplitude, but these changes did not occur until after the homeostatic recovery of embryonic activity. Therefore, a separate mechanism(s) existed that recovered embryonic activity. Here, we show that reducing excitatory GABAergic transmission also triggered a homeostatic increase in cellular excitability, which occurred more rapidly than quantal changes, and therefore could explain the recovery of embryonic activity. Cellular excitability was increased through an increase in sodium currents and the reduction of fast-inactivating and calcium-activated potassium currents. These changes in sodium and potassium currents have been shown to be critical for increasing excitability by modulating action potential waveform and firing frequency (21–23). Further, reducing these currents in ovo alters the rate of recovery of embryonic activity. Together, these findings support the idea that $GABA_A$ receptor signaling is a critical part of the machinery that senses lowered activity levels and triggers homeostatic changes in both cellular excitability and synaptic strength.

Compensatory changes in cellular excitability have been shown after activity blockade in invertebrate central pattern generators and mammalian central nervous system (1–3). Data from these diverse systems have shown that reducing activity triggers changes

in cellular excitability through modification of ionic conductances. Previous studies of vertebrate central synapses have shown homeostatic increases in sodium channel currents (8, 20), reductions in Ca^{2+}-activated potassium currents (16, 20), and reductions in the density and inactivation kinetics of transient potassium channels (14) after TTX-induced activity block. We have blocked $GABA_A$ transmission and see comparable results to these previous studies that block activity, suggesting a similar process has been triggered. However, in our study it is highly unlikely that reduced spontaneous network activity triggered these changes beyond simply reducing released GABA. Although we do see a transient reduction in SNA following injection of the $GABA_A$ receptor antagonist, the reduction in activity by itself does not trigger changes in cellular excitability, because the same transient reduction of activity occurs without any changes in cellular excitability following glutamate receptor block. Our findings therefore support the idea that compensatory changes in cellular excitability are triggered by lowered GABAergic neurotransmission rather than by activity or neurotransmission in general. Thus, in the developing spinal cord, GABA transmission appears to be sensed as a monitor of activity. In several previous studies it was not possible to separate the influence of activity from transmission. For instance, changes in cellular excitability have been identified when transmission is perturbed, but activity has also been altered in these studies (24, 25). In the crab stomatogastric ganglion, perturbation of neuromodulatory input, independent of spiking activity, appears to be critical to the homeostatic regulation of ionic conductances (26). At the neuromuscular junction, transmitter blockade has been shown to trigger retrograde changes in motoneuron cellular excitability (27, 28), and this was independent of cellular spiking activity (29). Reduced neurotransmission triggering synaptic scaling has been proposed previously (17, 30). Together, these findings support the role of ligand-gated channels in the sensing machinery that triggers changes in cellular excitability in the developing spinal cord, and possibly in other systems as well.

Our findings demonstrate a functionally economical process, because 3 homeostatic mechanisms (cellular excitability, as well as AMPAergic- and GABAergic-quantal strength) are all triggered via lowered $GABA_A$ receptor activation. Our data support a model in which $GABA_A$ receptors sense reductions in extracellular GABA as a proxy for activity, and this triggers increases in cellular excitability and quantal strength. This increase in synaptic strength could be triggered because $GABA_A$ receptors remain blocked throughout the 48-h period, thus simulating prolonged activity blockade. Interestingly, 48 h of $GABA_A$ receptor block resulted in a reduced cellular excitability compared with the 12-h block. Several possibilities could underlie this finding: (*i*) increasing quantal amplitude could feed back negatively on cellular excitability; (*ii*) the activity recovers and slightly surpasses normal levels of activity (Fig. 1*A*), and these slightly higher activity levels feedback negatively on cellular excitability; and (*iii*) it may be that the increases in cellular excitability are time-dependent and cannot be maintained through the 48-h treatment. The findings raise the possibility that there is a relationship between cellular excitability and quantal compensations. The importance of $GABA_A$ receptor signaling in triggering homeostatic mechanisms is not surprising, because $GABA_A$ transmission is depolarizing, can lead to calcium entry, and has been shown to be critical for several aspects of early development, including cell proliferation, migration, differentiation, establishment of synaptic connections, and synaptic refinement (31).

Blocking activity in networks of cultured neurons leads to compensatory increases in the intrinsic excitability of neurons (2, 3, 32) and increases in the strength of excitatory synaptic inputs (4, 5). Previous studies of this kind of synaptic and cellular homeostasis have shown that compensatory changes can be observed after 24–48 h of activity block (refs. 1, 2, 4, 30, and 33; however, see ref. 34). These changes in cellular excitability and synaptic strength are thought to contribute to the homeostatic recovery of normal activity levels. Only a few studies actually demonstrate a homeostatic recovery of original activity levels (6, 7, 35, 36). However, these studies do not compare the timing of recovery with the onset of the homeostatic mechanisms. One previous study using rat hippocampal slice in culture did find that changes in cellular excitability occur before the onset of changes in inhibitory synaptic strength, but again it was not clear when activity was recovered (7). In the present study, we have tested and subsequently found that changes in cellular excitability occurred during the period in which the activity was recovered and before changes in synaptic strength were engaged. This suggests the surprising possibility that cellular excitability is the mechanism that homeostatically recovers the activity, and that changes in quantal amplitude are not involved in this step of the homeostatic process. Here, we show that changes in voltage-gated channels respond quickly and recover activity, whereas slower-responding changes in the strength of synaptic inputs may serve to maintain or consolidate the increase in network excitability. This raises the intriguing possibility that changes in cellular excitability represent a first step that could trigger or be necessary for the slower changes in quantal amplitude.

After injection of glutamatergic receptor antagonists, embryonic movements return to control levels without triggering any sustained changes in cellular excitability or synaptic strength. Several possibilities could explain recovery following CNQX/APV treatment. (*i*) In the in vitro spinal cord, glutamate blockade delays the onset of the next episode of SNA, which leads to a transient chloride accumulation, strengthening GABAergic synaptic inputs (37, 38). It is likely that a transient accumulation of chloride also occurs in ovo following glutamate block. (*ii*) There could also be changes in the probability of release (39), which we have not measured. (*iii*) Finally, there could be transient changes in cellular excitability that occur in ovo that are not maintained in the isolated spinal preparation.

We have identified 2 homeostatic mechanisms with distinct temporal and functional roles in homeostatic plasticity. Recognition of this is critical to our understanding of the order and relationship of the molecular cascades that underlie the homeostatic process in the living embryo. It will be important for studies in other systems to examine the onset of cellular excitability and synaptic scaling in relation to the recovery of activity to determine whether our findings in the embryonic spinal cord represent a more general principle. Further, we show another example of the critical importance that the neurotransmitter GABA plays in early development. Here, GABA appears to act as a proxy for activity, which is sensed through the $GABA_A$ receptor and, when reduced, triggers coordinated compensatory changes in I_{Na}, I_A, $I_{K(Ca)}$, GABAergic, and AMPAergic quantal amplitude. Therefore, GABA signaling has profound effects on the maturation of cellular excitability and synaptic strength.

Experimental Procedures

In Ovo Pharmacological Blockade. Embryonic limb movements, which are a strong indicator of SNA experienced centrally, were monitored as described previously (17). Briefly, at stages 33–34 (E8) (40), a window in the shell was opened to allow monitoring of chicken embryo limb movements and drug application. SNA was quantified in ovo by counting the total time the chicken embryo moved during a 5-min period of observation. To block neurotransmission, an aqueous solution of gabazine (or SR 95531 hydrobromide; 10 μM, assume a 50-mL egg volume), CNQX (20 μM), APV (100 μM), or some combination of these antagonists was injected onto the chorioallantoic membrane of the chicken embryo. These concentrations were previously determined to be appropriate for blocking neurotransmission from E8 to E10 (17). To block potassium or sodium channels in ovo, an aqueous solution of gabazine (20 μM; Tocris Cookson) or saline (1 mL) was injected onto the E9.5 embryo, along with lidocaine (250 μM; Sigma–Aldrich) or 4-AP (0.1 μM; Sigma–Aldrich) and TEA (0.1 μM; Sigma–Aldrich).

Whole-Cell Electrophysiology. White Leghorn chicken embryos (Hy-Line Hatcheries) were dissected as described previously (41). Whole-cell voltage clamp and current clamp recordings were obtained from E10 motoneurons in the isolated in vitro chick spinal cord (*SI Methods*). Extracellular and intracellular solutions are provided in *SI Methods*.

Statistics. Data from averages are expressed as mean ± SEM. Significant differences were calculated by using Student's unpaired *t* test ($\alpha = 0.05$) when single comparisons were made. Differences between multiple groups were calculated by using 1-way ANOVA with posthoc Dunnett's test ($\alpha = 0.05$) or Tukey's test ($\alpha = 0.05$).

ACKNOWLEDGMENTS. We thank Dr. Astrid Prinz and Carlos Gonzalez-Islas for critical comments on the manuscript, and Danielle Schwartz for technical assistance. This research was supported by National Institute of Neurological Disorders and Stroke Grant NS-046510 and National Science Foundation Grant 0616097 (to P.W.), and National Institute of Neurological Disorders and Stroke Grant NS-057228 (to M.M.R.).

1. Davis GW (2006) Homeostatic control of neural activity: From phenomenology to molecular design. *Annu Rev Neurosci* 29:307–323.
2. Desai NS (2003) Homeostatic plasticity in the CNS: Synaptic and intrinsic forms. *J Physiol Paris* 97:391–402.
3. Marder EJ, Goaillard M (2006) Variability, compensation and homeostasis in neuron and network function. *Nat Rev Neurosci* 7:563–574.
4. Rich MM, Wenner P (2007) Sensing and expressing homeostatic synaptic plasticity. *Trends Neurosci* 30:119–125.
5. Turrigiano GG (2008) The self-tuning neuron: Synaptic scaling of excitatory synapses. *Cell* 135:422–435.
6. Turrigiano GG, Leslie KR, Desai NS, Rutherford LC, Nelson SB (1998) Activity-dependent scaling of quantal amplitude in neocortical neurons. *Nature* 391:892–896.
7. Karmarkar UR, Buonomano DV (2006) Different forms of homeostatic plasticity are engaged with distinct temporal profiles. *Eur J Neurosci* 23:1575–1584.
8. Aptowicz, CO, Kunkler PE, Kraig RP (2004) Homeostatic plasticity in hippocampal slice cultures involves changes in voltage-gated Na+ channel expression. *Brain Res* 998:155–163.
9. Gonzalez-Islas C, Wenner P (2006) Spontaneous network activity in the embryonic spinal cord regulates AMPAergic and GABAergic synaptic strength. *Neuron* 49:563–575.
10. Feller MB (1999) Spontaneous correlated activity in developing neural circuits. *Neuron* 22:653–656.
11. O'Donovan MJ (1999) The origin of spontaneous activity in developing networks of the vertebrate nervous system. *Curr Opin Neurobiol* 9:94–104.
12. Ben-Ari Y (2001) Developing networks play a similar melody. *Trends Neurosci* 24:353–360.
13. O'Donovan MJ, Chub N, Wenner P (1998) Mechanisms of spontaneous activity in developing spinal networks. *J Neurobiol* 37:131–145.
14. Casavant RH, Colbert CM, Dryer SE (2004) A-current expression is regulated by activity but not by target tissues in developing lumbar motoneurons of the chick embryo. *J Neurophysiol* 92:2644–2651.
15. Hanson MG, Landmesser LT (2004) Normal patterns of spontaneous activity are required for correct motor axon guidance and the expression of specific guidance molecules. *Neuron* 43:687–701.
16. Martin-Caraballo M, Dryer SE (2002) Activity- and target-dependent regulation of large-conductance Ca2+-activated K+ channels in developing chick lumbar motoneurons. *J Neurosci* 22:73–81.
17. Wilhelm JC, Wenner P (2008) GABAA transmission is a critical step in the process of triggering homeostatic increases in quantal amplitude. *Proc Natl Acad Sci USA* 105:11412–11417.
18. Turrigiano G, Abbott LF, Marder E (1994) Activity-dependent changes in the intrinsic properties of cultured neurons. *Science* 264:974–977.
19. Turrigiano G, LeMasson G, Marder E. (1995) Selective regulation of current densities underlies spontaneous changes in the activity of cultured neurons. *J Neurosci* 15:3640–3652.
20. Desai NS, Rutherford LC, Turrigiano GG (1999) Plasticity in the intrinsic excitability of cortical pyramidal neurons. *Nat Neurosci* 2:515–520.
21. McCobb DP, Best PM, Beam KG (1990) The differentiation of excitability in embryonic chick limb motoneurons. *J Neurosci* 10:2974–2984.
22. Martin-Caraballo M, Greer JJ (2000) Development of potassium conductances in perinatal rat phrenic motoneurons. *J Neurophysiol* 83:3497–3508.
23. Gao BX, Ziskind-Conhaim L (1998) Development of ionic currents underlying changes in action potential waveforms in rat spinal motoneurons. *J Neurophysiol* 80:3047–3061.
24. Weston AJ, Baines RA (2007) Translational regulation of neuronal electrical properties. *Invert Neurosci* 7:75–86.
25. Brickley SG, Revilla V, Cull-Candy SG, Wisden W, Farrant M (2001) Adaptive regulation of neuronal excitability by a voltage-independent potassium conductance. *Nature* 409:88–92.
26. Khorkova O, Golowasch J (2007) Neuromodulators, not activity, control coordinated expression of ionic currents. *J Neurosci* 27:8709–8718.
27. Nakanishi ST, Cope TC, Rich MM, Carrasco DI, Pinter MJ (2005) Regulation of motoneuron excitability via motor endplate acetylcholine receptor activation. *J Neurosci* 25:2226–2232.
28. Nick TA, Ribera AB (2000) Synaptic activity modulates presynaptic excitability. *Nat Neurosci* 3:142–149.
29. Bichler EK, et al. (2007) Enhanced transmission at a spinal synapse triggered in vivo by an injury signal independent of altered synaptic activity. *J Neurosci* 27:12851–12859.
30. Stellwagen D, Malenka RC (2006) Synaptic scaling mediated by glial TNF-alpha. *Nature* 440:1054–1059.
31. Ben-Ari Y, Gaiarsa JL, Tyzio R, Khazipov R (2007) GABA: A pioneer transmitter that excites immature neurons and generates primitive oscillations. *Physiol Rev* 87:1215–1284.
32. Schulz DJ (2006) Plasticity and stability in neuronal output via changes in intrinsic excitability: It's what's inside that counts. *J Exp Biol* 209:4821–4827.
33. Turrigiano G (2007) Homeostatic signaling: The positive side of negative feedback. *Curr Opin Neurobiol* 17:318–324.
34. Ibata K, Sun Q, Turrigiano GG (2008) Rapid synaptic scaling induced by changes in postsynaptic firing. *Neuron* 57:819–826.
35. Burrone J, O'Byrne M, Murthy VN (2002) Multiple forms of synaptic plasticity triggered by selective suppression of activity in individual neurons. *Nature* 420:414–418.
36. Pratt KG, Aizenman CD (2007) Homeostatic regulation of intrinsic excitability and synaptic transmission in a developing visual circuit. *J Neurosci* 27:8268–8277.
37. Chub N, O'Donovan MJ (1998) Blockade and recovery of spontaneous rhythmic activity after application of neurotransmitter antagonists to spinal networks of the chick embryo. *J Neurosci* 18:294–306.
38. Chub N, O'Donovan MJ (2001) Post-episode depression of GABAergic transmission in spinal neurons of the chick embryo. *J Neurophysiol* 85:2166–2176.
39. Frank CA, Kennedy MJ, Goold CP, Marek KW, Davis GW (2006) Mechanisms underlying the rapid induction and sustained expression of synaptic homeostasis. *Neuron* 52:663–677.
40. Hamburger V, Hamilton HC (1951) A series of normal stages in the development of the chick embryo. *J Morphol* 88:49–92.
41. Wenner P, O'Donovan MJ (2001) Mechanisms that initiate spontaneous network activity in the developing chick spinal cord. *J Neurophysiol* 86:1481–1498.